

# Hadronic Higgs Production with Heavy Quarks at the Tevatron and the LHC \*

S. Dawson<sup>†</sup> and C. B. Jackson<sup>‡</sup>

*Physics Department, Brookhaven National Laboratory, Upton, N.Y. USA*

L. Reina<sup>§</sup>

*Physics Department, Florida State University, Tallahassee, FL 32306-4350, USA*

D. Wackerth<sup>¶</sup>

*Department of Physics, SUNY at Buffalo, Buffalo, NY 14260-1500, USA*

## Abstract

We review the status of the QCD corrected cross sections and kinematic distributions for the production of a Higgs boson in association with top quark or bottom quark pairs at the Fermilab Tevatron and at the LHC. Results for  $b\bar{b}H$  production are presented in the Minimal Supersymmetric Model, where the rates can be greatly enhanced relative to the Standard Model rates. We place particular emphasis on theoretical uncertainties due to renormalization and factorization scale dependence and on the uncertainties coming from the Parton Distribution Functions.

## 1 Introduction

A light Higgs boson is preferred by precision fits of the Standard Model (SM) and also theoretically required by the Minimal Supersymmetric extension of the Standard Model (MSSM). The production of a Higgs boson in association with a heavy quark and antiquark pair, both  $t\bar{t}$  and  $b\bar{b}$ , at the Tevatron and the Large Hadron Collider (LHC) will be sensitive to the Higgs-fermion couplings and can help discriminate between models.

---

\*Prepared for the TeV4LHC Higgs Working Group Report.

<sup>†</sup>dawson@bnl.gov

<sup>‡</sup>jackson@quark.phy.bnl.gov

<sup>§</sup>reina@hep.fsu.edu

<sup>¶</sup>dow@ubpheno.physics.buffalo.edu

The associated production of a Higgs boson with a pair of  $t\bar{t}$  quarks has a distinctive signature and can give a direct measurement of the top quark Yukawa coupling. This process is probably not observable at the Tevatron, but will be a discovery channel at the LHC for  $M_h < 130$  GeV. The associated production of a Higgs boson with a pair of  $b\bar{b}$  quarks has a small cross section in the Standard Model, and can be used to test the hypothesis of enhanced bottom quark Yukawa couplings in the MSSM with large values of  $\tan\beta$ . Both the Tevatron and the LHC will be able to search for enhanced  $b\bar{b}h$  production, looking for a final state containing no bottom quarks (inclusive production), one bottom quark (semi-inclusive production) or two bottom quarks (exclusive production).

The rates for  $t\bar{t}h$  production at the Tevatron and the LHC have been calculated at NLO QCD several years ago[1, 2, 3, 4, 5, 6]. The theoretical predictions for  $b\bar{b}h$  production at hadron colliders involve several subtle issues, and depend on the number of bottom quarks identified in the final state. In the case of no or only one tagged bottom quark there are two approaches available for calculating the cross sections for  $b\bar{b}h$  production, called the four flavor number schemes (4FNS)[7, 8] and five flavor number scheme (5FNS)[9]. The main difference between these two approaches is that the 4FNS is a fixed-order calculation of QCD corrections to the  $gg$  and  $q\bar{q}$ -induced  $b\bar{b}h$  production processes, while in the 5FNS the leading processes arise from  $bg$  ( $\bar{b}g$ ) and  $b\bar{b}$  initial states and large collinear logarithms are resummed using a perturbatively defined bottom quark Parton Distribution Function (PDF). Very good agreement is found for the NLO QCD corrected cross sections for  $b\bar{b}$  Higgs associated production when the two schemes are compared[10, 11].

In the following sections, we present numerical results at NLO QCD for  $t\bar{t}h$  and  $b\bar{b}h$  production at the Tevatron and the LHC. If not stated otherwise, numerical results have been obtained in the 4FNS. We emphasize theoretical uncertainties from scale and PDF uncertainties and also present differential cross sections at NLO for  $b\bar{b}h$  production in the case when two  $b$  quarks are tagged.

## 2 Results for $t\bar{t}h$ Production

The observation of a  $t\bar{t}h$  final state will allow for the measurement of the  $t\bar{t}h$  Yukawa coupling. If  $M_h \leq 130$  GeV,  $pp \rightarrow t\bar{t}h$  is an important discovery channel for a SM-like Higgs boson at the LHC ( $\sqrt{s} = 14$  TeV) [12, 13]. Given the statistics expected at the LHC,  $pp \rightarrow t\bar{t}h$ , with  $h \rightarrow b\bar{b}, \tau^+\tau^-, W^+W^-, \gamma\gamma$  will be instrumental for the determination of the couplings of the Higgs boson. Precisions of the order of 10-15% on the measurement of the top quark Yukawa coupling can be obtained with integrated luminosities of  $100 \text{ fb}^{-1}$  per detector[14, 15, 16, 17].

The impact of NLO QCD corrections on the total cross section for  $p\bar{p}, pp \rightarrow t\bar{t}h$  production in the Standard Model is illustrated in Fig. 1[6, 5, 1, 3] and Fig. 2[6, 3].

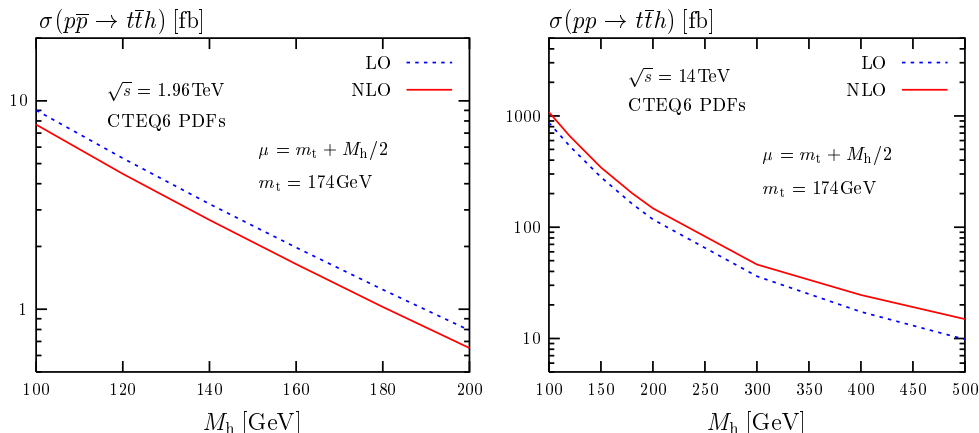


Figure 1: Total LO and NLO cross sections for  $pp, p\bar{p} \rightarrow t\bar{t}h$  as functions of  $M_h$ , at  $\sqrt{s}=1.96$  TeV and  $\sqrt{s}=14$  TeV, for  $\mu = m_t + M_h/2$ .

The dependence of the total cross sections on the renormalization and factorization scales is strongly reduced at NLO as shown in Fig. 2. The numerical results at NLO are obtained using CTEQ4M (Fig. 2 (l.h.s.)), CTEQ5M (Fig. 2 (r.h.s.)), and CTEQ6M (Fig. 1) parton distribution functions. The NLO cross section is evaluated using the 2-loop evolution of  $\alpha_s(\mu)$  with  $\alpha_s^{NLO}(M_Z) = 0.116$  (Fig. 2 (l.h.s.)) and  $\alpha_s^{NLO}(M_Z) = 0.118$  (Fig. 2 (r.h.s.)) and Fig. 1), and  $m_t = 174$  GeV. The renormalization/factorization scale dependence, uncertainty on the PDFs, and the error on the top quark pole mass,  $m_t$ , are estimated to give a 15-20% uncertainty.

### 3 Results for $b\bar{b}h$ Production

The  $b\bar{b}h$  production processes are only relevant discovery modes in the MSSM with large  $\tan\beta$ . To a good approximation, the predictions for the MSSM rates can easily be derived from the Standard Model results by rescaling the Yukawa couplings[10]. The dominant MSSM radiative correction to  $b\bar{b}h$  production can be taken into account by including the MSSM corrections to the  $b\bar{b}h$  vertex only, i.e. by replacing the tree level Yukawa couplings by the radiative corrected ones. We follow the treatment of the program FEYNHIGGS [18, 19] and take into account the leading,  $\tan\beta$  enhanced, radiative corrections that are generated by gluino-sbottom and chargino-stop loops. For large  $\tan\beta$ , the bottom quark Yukawa coupling is enhanced and the top quark Yukawa coupling is strongly suppressed, resulting in a MSSM  $b\bar{b}h$  cross section that is about three orders of magnitude larger than the Standard Model cross section. For the Tevatron, we calculate the production rates for the lightest MSSM Higgs boson,  $h^0$ , while for the LHC we consider the rate for the heavier neutral Higgs

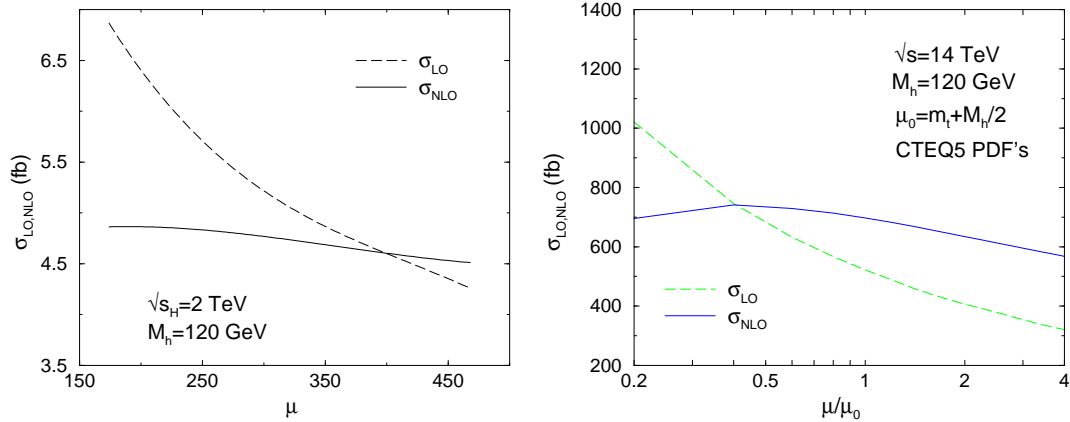


Figure 2: Dependence of  $\sigma_{LO,NLO}(pp, p\bar{p} \rightarrow t\bar{t}h)$  on the renormalization/factorization scale  $\mu$ , at  $\sqrt{s}=2$  TeV (l.h.s.) and  $\sqrt{s}=14$  TeV (r.h.s.), for  $M_h=120$  GeV.

boson,  $H^0$ .<sup>1</sup>

In the numerical evaluation of cross sections for the exclusive and semi-inclusive channels ( $b\bar{b}h$  and  $bh + \bar{b}h$  production), it is required that the final state bottom quarks have  $p_T > 20$  GeV and pseudorapidity  $|\eta| < 2.0$  for the Tevatron and  $|\eta| < 2.5$  for the LHC. In the NLO real gluon emission contributions, the final state gluon and bottom quarks are considered as separate particles only if their separation in the pseudorapidity-azimuthal angle plane,  $\Delta R = \sqrt{(\Delta\eta)^2 + (\Delta\phi)^2}$ , is larger than 0.4. For smaller values of  $\Delta R$ , the four momentum vectors of the two particles are combined into an effective bottom/anti-bottom quark momentum four-vector.

If not stated otherwise, the numerical results at NLO are obtained using CTEQ6M PDFs, the 2-loop evolution of  $\alpha_s(\mu)$  with  $\alpha_s^{NLO}(M_Z) = 0.118$ , and the  $\overline{MS}$  renormalization scheme for the bottom quark mass and Yukawa coupling with 2-loop renormalization group improved  $\overline{MS}$  masses. The bottom quark pole mass is chosen to be  $m_b = 4.62$  GeV.

### 3.1 Total Cross Sections for $b\bar{b}h$ Production

We present total cross section results at NLO in the 4FNS in Fig. 3 for associated  $b\bar{b}$  Higgs production in the MSSM with  $\tan\beta = 40$ . The bands represent the theoretical uncertainty due to the residual scale dependence. They have been obtained by varying

<sup>1</sup>We assume  $M_{SUSY} = 1$  TeV,  $M_{\tilde{g}} = 1$  TeV,  $A_b = A_t = 2$  TeV ( $h^0$ ),  $A_b = A_t = 25$  GeV ( $H^0$ ),  $\mu = M_2 = 200$  GeV ( $h^0$ ), and  $\mu = M_2 = 1$  TeV ( $H^0$ ). For  $M_{h^0} = 120$  GeV, the  $bbh^0$  coupling is enhanced by a factor of 33 relative to the SM coupling, while for  $M_{H^0}$  between 200 and 800 GeV, the  $bbH^0$  coupling is enhanced by a factor of 27 relative to the SM coupling.

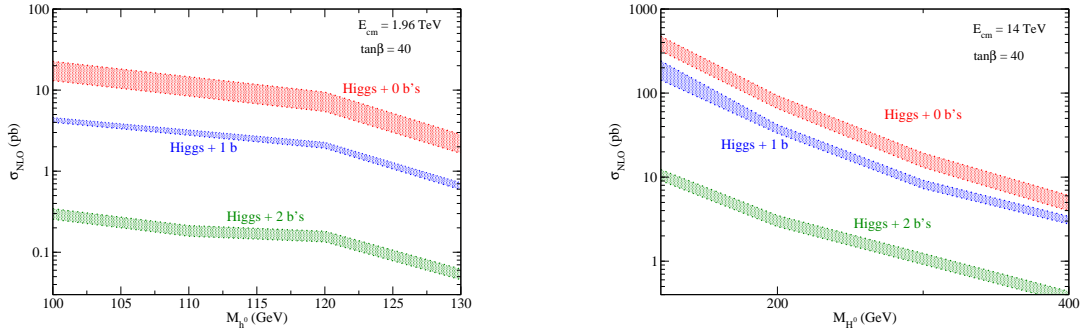


Figure 3: Total cross sections for  $pp, p\bar{p} \rightarrow b\bar{b}h$  in the MSSM in the 4FNS at NLO for the Tevatron and the LHC in the MSSM with  $\tan\beta = 40$  and with 0,1 or 2  $b$  quarks identified. The Tevatron (LHC) plot is for the lightest (heaviest) neutral Higgs boson,  $h^0$  ( $H^0$ ). The error bands have been obtained by varying the renormalization and factorization scales as described in the text.

the renormalization ( $\mu_r$ ) and factorization ( $\mu_f$ ) scales independently from  $\mu_0/4$  to  $\mu_0$ , where  $\mu_0 = m_b + M_{H^0}/2$ .

If the outgoing bottom quarks cannot be observed then the dominant MSSM Higgs production process at large  $\tan\beta$  is  $gg \rightarrow (b\bar{b})h$  (the curve labelled '0 b'). The inclusive cross section is experimentally relevant only if the Higgs boson can be detected above the background without tagging bottom quarks. At the LHC, this process can be identified at large  $\tan\beta$  by the decays to  $\mu^+\mu^-$  and  $\tau^+\tau^-$  for the heavy Higgs bosons,  $H^0$  and  $A^0$ , of the MSSM. At the Tevatron this process, with  $h^0 \rightarrow \tau^+\tau^-$ , has been used to search for the neutral MSSM Higgs boson. If a single bottom quark is tagged then the final state is  $bh$  or  $\bar{b}h$  (the curve labelled '1 b'). Although requiring a  $b$  quark in the final state significantly reduces the rate, it also reduces the background. A recent Tevatron study [20] used the search for neutral MSSM Higgs bosons in events with three bottom quarks in the final state ( $bh^0 + \bar{b}h^0$  production with  $h^0 \rightarrow b\bar{b}$ ) to impose limits on the  $\tan\beta$  and  $M_{A^0}$  parameter space.

Finally, we show the fully exclusive cross sections for  $b\bar{b}h$  production, where both the outgoing  $b$  and  $\bar{b}$  quarks are identified (the curve labelled '2 b'). The exclusive measurement corresponds to the smallest cross section, but it also has a significantly reduced background. Moreover, both the exclusive and semi-inclusive  $b\bar{b}h$  production modes are the only ones that can unambiguously measure the bottom quark Yukawa coupling.

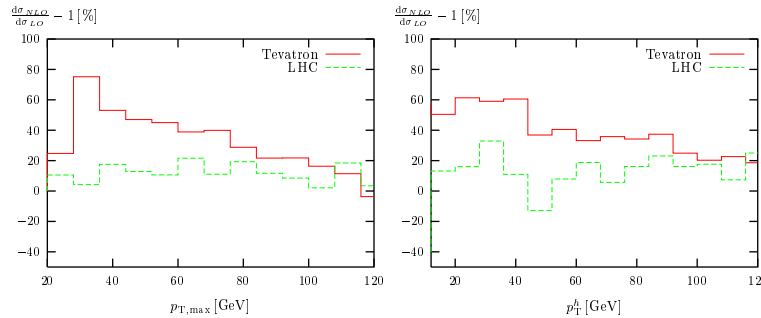


Figure 4: The relative corrections  $d\sigma_{NLO}/d\sigma_{LO} - 1$  for the  $p_T$  distribution of the bottom or anti-bottom quark with the largest  $p_T$  ( $p_{T,max}$ ) (left) and of the SM Higgs boson ( $p_T^h$ ) (right) to  $b\bar{b}h$  production in the SM at the Tevatron (with  $\sqrt{s} = 2$  TeV and  $\mu = 2\mu_0$ ) and the LHC (with  $\sqrt{s} = 14$  TeV and  $\mu = 4\mu_0$ ).

### 3.2 Differential Cross Sections for $b\bar{b}h$ Production

In assessing the impact of the NLO corrections it is particularly interesting to study the kinematic distributions. In Figs. 4 and 5 we illustrate the impact of NLO QCD corrections on the transverse momentum and pseudorapidity distribution of the SM Higgs boson and the bottom quark by showing the relative correction,  $d\sigma_{NLO}/d\sigma_{LO} - 1$  (in percent) for the exclusive case ( $b\bar{b}h$  where both  $b$  quarks are observed). For the renormalization/factorization scale we choose  $\mu = 2\mu_0$  at the Tevatron and  $\mu = 4\mu_0$  at the LHC, with  $\mu_0 = m_b + M_h/2$ , and use the CTEQ5 set of PDFs. As can be seen, the NLO QCD corrections can considerably affect the shape of kinematic distributions, and their effect cannot be obtained from simply rescaling the LO distributions with a K-factor of  $\sigma_{NLO}/\sigma_{LO} = 1.38 \pm 0.02$  (Tevatron,  $\mu = 2\mu_0$ ) and  $\sigma_{NLO}/\sigma_{LO} = 1.11 \pm 0.03$  (LHC,  $\mu = 4\mu_0$ ).<sup>2</sup>

### 3.3 PDF and Renormalization/Factorization Scale Uncertainties

A major source of theoretical uncertainty for cross section predictions comes from the PDFs. We study the uncertainties of semi-inclusive  $bh$  production rates from the uncertainties in the PDFs using the CTEQ PDF sets[21]. First, the central value cross section  $\sigma_0$  is calculated using the global minimum PDF (i.e. CTEQ6M). The calculation of the cross section is then performed with the additional 40 sets of PDFs to produce 40 different predictions,  $\sigma_i$ . For each of these, the deviation from the central value is calculated to be  $\Delta\sigma_i^\pm = |\sigma_i - \sigma_0|$  when  $\sigma_i \gtrless \sigma_0$ . Finally, to

<sup>2</sup>The kinematic distributions have been calculated within the Standard Model and using the on-shell scheme for the definition of the  $b$  quark mass, but we see a similar behavior when using the  $\overline{MS}$  bottom quark Yukawa coupling.

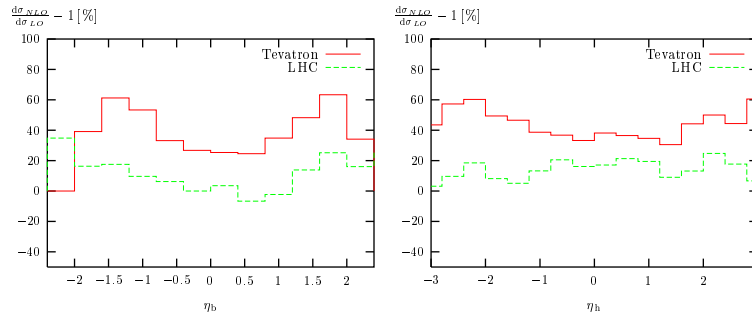


Figure 5: The relative corrections  $d\sigma_{NLO}/d\sigma_{LO} - 1$  for the  $\eta$  distribution of the bottom quark  $\eta_b$  (left) and of the SM Higgs boson ( $\eta_h$ ) (right) to  $b\bar{b}h$  production in the SM at the Tevatron (with  $\sqrt{s}=2$  TeV and  $\mu=2\mu_0$ ) and the LHC (with  $\sqrt{s}=14$  TeV and  $\mu=4\mu_0$ ).

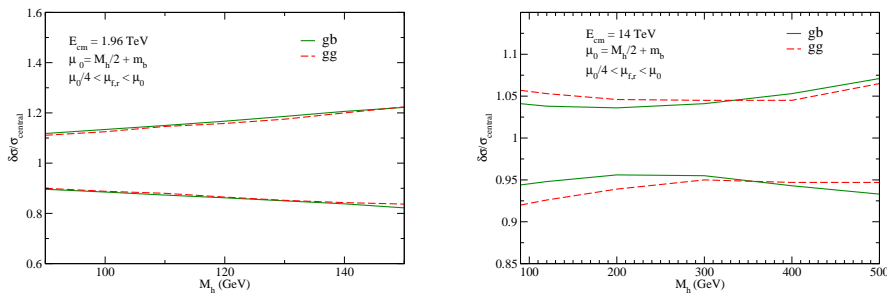


Figure 6: Normalized cross sections for Higgs production with one  $b$  jet at the Tevatron (l.h.s) and the LHC (r.h.s) showing the uncertainty from PDFs for both the  $gg$  (4FNS) and  $bg$  (5FNS) initial states.

obtain the uncertainties due to the PDFs the deviations are summed quadratically as  $\Delta\sigma^\pm = \sqrt{\sum_i \Delta\sigma_i^{\pm 2}}$  and the cross section including the theoretical uncertainties arising from the PDFs is quoted as  $\sigma_0|_{-\Delta\sigma^-}^{+\Delta\sigma^+}$ .

In Fig. 6, we plot the normalized total SM NLO cross sections for semi-inclusive  $bh$  production, calculated in the 5FNS ( $bg \rightarrow bh$ ) as implemented in MCFM [22] and in the 4FNS ( $gg \rightarrow b(\bar{b})h$ ), and compare their respective uncertainties due to the PDFs. We see that, at both the Tevatron and the LHC, the PDF uncertainties are almost identical for both the  $gg$  and  $bg$  initial states.

In Figs. 7 and 8 we compare the uncertainties from residual scale dependence and the PDFs on the example of  $bg \rightarrow bh$  (5FNS) at the Tevatron and LHC respectively[10]. Here, we perform the comparison for both the total cross section (left) and the to-

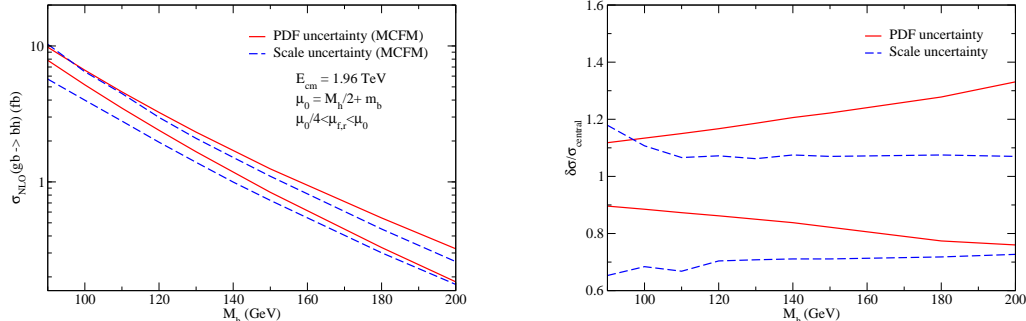


Figure 7: Comparison between theoretical uncertainties due to scale dependence and uncertainties arising from the PDFs at the Tevatron for semi-inclusive  $bh$  production in the Standard Model. In the right-hand plot, both uncertainty bands have been normalized to the central value of the total cross section  $\sigma_0$ .

tal cross section normalized to the central value calculated with CTEQ6M (right). Similar results are obtained in the 4FNS.

From Fig. 8 one can see that, at the LHC, the theoretical uncertainty is dominated by the residual scale dependence. Due to the large center of mass (c.o.m.) energy of the LHC, the gluons and bottom quarks in the initial state have small momentum fraction ( $x$ ) values and, hence, small PDF uncertainties typically in the 5-10% range.

In contrast, due to the smaller c.o.m. energy, the PDF uncertainties at the Tevatron (Fig. 7) are comparable and even larger than the uncertainties due to residual scale dependence over the full Higgs mass range. The smaller c.o.m. energy results in higher- $x$  gluons and bottom quarks in the initial state which corresponds to large PDF uncertainties in the 10-30% range.

## 4 Conclusion

The NLO cross sections for  $t\bar{t}h$  and  $b\bar{b}h$  have been presented for the Tevatron and the LHC with emphasis on the renormalization/factorization scale and PDF dependences.

## Acknowledgments

The work of S.D. and C.J. (L.R) is supported in part by the U.S. Department of Energy under grant DE-AC02-98CH10886 (DE-FG-02-91ER40685). The work of

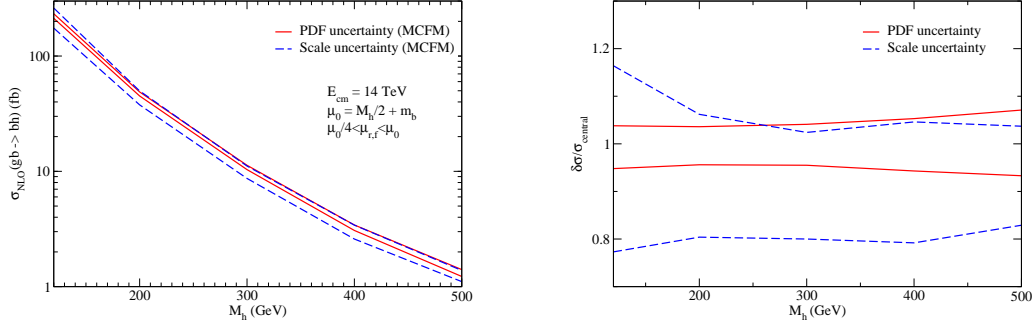


Figure 8: Comparison between theoretical uncertainties due to scale dependence and uncertainties arising from the PDFs at the LHC for semi-inclusive  $bh$  production in the Standard Model. In the bottom plot, both uncertainty bands have been normalized to the central value of the total cross section  $\sigma_0$ .

D.W. is supported in part by the National Science Foundation under grant No. PHY-0244875.

## References

- [1] Reina, L., and Dawson, S., *Phys. Rev. Lett.*, **87**, 201804 (2001).
- [2] Beenakker, W., Dittmaier, S., Krämer, M., Plümper, B., Spira, M., and Zerwas, P., *Phys. Rev. Lett.*, **87**, 201805 (2001).
- [3] Reina, L., Dawson, S., and Wackerroth, D., *Phys. Rev.*, **D65**, 053017 (2002).
- [4] Beenakker, W., Dittmaier, S., Krämer, M., Plümper, B., Spira, M., and Zerwas, P., *Nucl. Phys.*, **B653**, 151–203 (2003).
- [5] Dawson, S., Orr, L. H., Reina, L., and Wackerroth, D., *Phys. Rev.*, **D67**, 071503 (2003).
- [6] Dawson, S., Jackson, C., Orr, L. H., Reina, L., and Wackerroth, D., *Phys. Rev.*, **D68**, 034022 (2003).
- [7] Dittmaier, S., Kramer, M., and Spira, M., *Phys. Rev.*, **D70**, 074010 (2004).
- [8] Dawson, S., Jackson, C. B., Reina, L., and Wackerroth, D., *Phys. Rev. Lett.*, **94**, 031802 (2005).

- 
- [9] Maltoni, F., Sullivan, Z., and Willenbrock, S., *Phys. Rev.*, **D67**, 093005 (2003).
- [10] Dawson, S., Jackson, C. B., Reina, L., and Wackerroth, D., *Mod. Phys. Lett.*, **A21**, 89–110 (2006).
- [11] Campbell, J., et al., *hep-ph/0405302* (2004).
- [12] Beneke, M., et al., *hep-ph/0003033* (2000).
- [13] Drollinger, V., *Proceedings of Workshop on Physics at TeV Colliders, Les Houches, France, 21 May - 1 Jun 2001* (2001).
- [14] Zeppenfeld, D., Kinnunen, R., Nikitenko, A., and Richter-Was, E., *Phys. Rev.*, **D62**, 013009 (2000).
- [15] Belyaev, A., and Reina, L., *JHEP*, **08**, 041 (2002).
- [16] Maltoni, F., Rainwater, D. L., and Willenbrock, S., *Phys. Rev.*, **D66**, 034022 (2002).
- [17] Duhrssen, M., et al., *hep-ph/0407190* (2004).
- [18] Hahn, T., Heinemeyer, S., Hollik, W., and Weiglein, G., *webpage: www.feynhiggs.de (Version 2.2.10) (????)*.
- [19] Hahn, T., Heinemeyer, S., Hollik, W., and Weiglein, G., *Proceedings of 3rd Les Houches Workshop: Physics at TeV Colliders, Les Houches, France, 26 May - 6 Jun 2003* (2003).
- [20] Abazov, V. M., et al., *Phys. Rev. Lett.*, **95**, 151801 (2005).
- [21] Pumplin, J., et al., *JHEP*, **07**, 012 (2002).
- [22] Campbell, J., and Ellis, R., *webpage: mcfm.fnal.gov (????)*.

# 1 Hadronic Higgs Production with Heavy Quarks at the Tevatron and the LHC

## 1.1 Introduction

A light Higgs boson is preferred by precision fits of the Standard Model (SM) and also theoretically required by the Minimal Supersymmetric extension of the Standard Model (MSSM). Searches at both the Tevatron and the Large Hadron Collider (LHC) will play a crucial role in discriminating between models. In this context, the production of a Higgs boson in association with a heavy quark and antiquark pair, both  $t\bar{t}$  and  $b\bar{b}$ , plays a very important role.

The associated production of a Higgs boson with a pair of  $t\bar{t}$  quarks has a distinctive signature, and can give a direct measurement of the top quark Yukawa coupling. This process is probably not observable at the Tevatron, but will be a discovery channel at the LHC for  $M_h < 130 \text{ GeV}$ . The associated production of a Higgs boson with a pair of  $b\bar{b}$  quarks has a small cross section in the Standard Model, and can be used to test the hypothesis of enhanced bottom quark Yukawa couplings in the MSSM with large values of  $\tan\beta$ . Both the Tevatron and the LHC will be able to search for enhanced  $b\bar{b}h$  production, looking for a final state containing no bottom quarks (inclusive production), one bottom quark (semi-inclusive production) or two bottom quarks (exclusive production).

The theoretical prediction for the  $b\bar{b}h$  production rate at hadron colliders involves several subtle issues, and depends on the number of bottom quarks identified in the final state. In the case of no or only one tagged bottom quark there are two approaches available for calculating the cross sections for  $b\bar{b}h$  production, called the four flavor (4FNS) and five flavor (5FNS) number schemes. The main difference between these two approaches is that the 4FNS is a fixed-order calculation of QCD corrections to the  $gg$  and  $q\bar{q}$ -induced  $b\bar{b}h$  production processes, while in the 5FNS the leading processes arise from  $bg$  ( $\bar{b}g$ ) and  $b\bar{b}$  initial states and large collinear logarithms are resummed using a perturbatively defined bottom quark Parton Distribution Function (PDF). The NLO QCD corrected cross sections for  $b$  Higgs associated production are in excellent agreement in when the two schemes are compared.

In the following sections, we present NLO numerical results for  $t\bar{t}h$  and  $b\bar{b}h$  production at the Tevatron and the LHC. We emphasize theoretical uncertainties from scale and PDF uncertainties and also present differential cross sections at NLO.

## 1.2 Results for $t\bar{t}h$ Production

The observation of a  $t\bar{t}h$  final state will allow for the measurement of the  $t\bar{t}h$  Yukawa coupling. Observing  $p\bar{p} \rightarrow t\bar{t}h$  at the Tevatron ( $\sqrt{s} = 1.96 \text{ TeV}$ ) will require very high luminosity and will probably be beyond the machine capabilities. On the other hand,

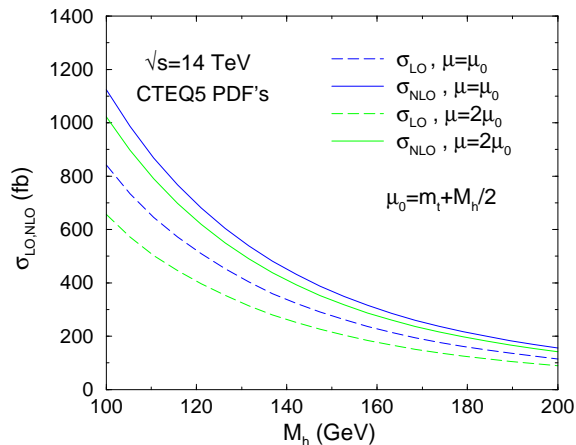


Figure 1:  $\sigma_{NLO}(pp \rightarrow t\bar{t}h)$  and  $\sigma_{LO}(pp \rightarrow t\bar{t}h)$  as functions of  $M_h$ , at  $\sqrt{s}=14$  TeV, for  $\mu = m_t + M_h/2$  and  $\mu = 2m_t + M_h$ .

if  $M_h \leq 130$  GeV,  $pp \rightarrow t\bar{t}h$  is an important discovery channel for a SM-like Higgs boson at the LHC ( $\sqrt{s}=14$  TeV) [? ? ?]. Given the statistics expected at the LHC,  $pp \rightarrow t\bar{t}h$ , with  $h \rightarrow b\bar{b}, \tau^+\tau^-, W^+W^-, \gamma\gamma$  will be instrumental for the determination of the couplings of the Higgs boson [? ? ? ?]. Several studies show that precisions of the order of 10-15% on the measurement of the top quark Yukawa coupling can be obtained with integrated luminosities of  $100 \text{ fb}^{-1}$  per detector.

The impact of NLO QCD corrections on the total cross section for  $pp \rightarrow t\bar{t}h$  production in the Standard Model is illustrated in Fig. 1.[? ? ? ?] The numerical results are obtained using CTEQ6M parton distribution functions. The NLO cross section is evaluated using the 2-loop evolution of  $\alpha_s(\mu)$  with  $\alpha_s^{NLO}(M_Z) = 0.118$  and  $M_t = 172 \text{ GeV}$ . The renormalization/factorization scale dependence is estimated to give a ?-?% uncertainty.

### 1.3 $b\bar{b}h$ Production

The  $b\bar{b}h$  processes are only relevant discovery modes in the MSSM with large  $\tan\beta$ . The predictions for the MSSM rates can easily be derived from the Standard Model results by rescaling the Yukawa couplings. The dominant MSSM radiative correction to  $b\bar{b}h$  production can be taken into account by including the MSSM corrections to the  $b\bar{b}h$  vertex only, i.e. by replacing the tree level Yukawa couplings by the radiative corrected ones. We follow the treatment of the program FEYNHIGGS [?] and take into account the leading,  $\tan\beta$  enhanced, radiative corrections that are generated by gluino-sbottom and chargino-stop loops. For large  $\tan\beta$ , the bottom Yukawa coupling is enhanced and the top Yukawa coupling is strongly suppressed, resulting in a MSSM  $b\bar{b}h$  cross section that is about three orders of magnitude larger than the

Standard Model cross section. For the Tevatron, we calculate the production rates for the lightest MSSM Higgs boson,  $h^0$ , while for the LHC we consider the rate for the heavier neutral Higgs boson,  $H^0$ .<sup>1</sup>

## Numerical Results for $b\bar{b}h$

For the exclusive and semi-inclusive channels ( $b\bar{b}h$  and  $bh + \bar{b}h$  production), it is required that the final state bottom quarks have  $p_T > 20$  GeV and pseudorapidity  $|\eta| < 2.0$  for the Tevatron and  $|\eta| < 2.5$  for the LHC. In the NLO real gluon emission contributions, the final state gluon and bottom quarks are considered as separate particles only if their separation in the pseudorapidity-azimuthal angle plane,  $\Delta R = \sqrt{(\Delta\eta)^2 + (\Delta\phi)^2}$ , is larger than 0.4. For smaller values of  $\Delta R$ , the four momentum vectors of the two particles are combined into an effective bottom/anti-bottom quark momentum four-vector.

## Total cross sections for $b\bar{b}h$ production

We present total cross section results at NLO in the 4FNS in Fig. 2 for associated  $b$  quark Higgs production in the MSSM with  $\tan\beta = 40$ . The bands represent the theoretical uncertainty due to the residual scale dependence. They have been obtained by varying the renormalization ( $\mu_r$ ) and factorization ( $\mu_f$ ) scales independently from  $\mu_0/4$  to  $\mu_0$ , where  $\mu_0 = m_b + M_h/2$ .

If the outgoing bottom quarks cannot be observed then the dominant MSSM Higgs production process at large  $\tan\beta$  is  $gg \rightarrow (b\bar{b})h$  (the curve labelled '0 b'). The exclusive measurement corresponds to the smallest cross section, but it also has a significantly reduced background. At the LHC, this process can be identified by the decays to  $\mu^+\mu^-$  and  $\tau^+\tau^-$  for the heavy Higgs bosons,  $H^0$  and  $A^0$ , of the MSSM. At the Tevatron this process, with  $h^0 \rightarrow \tau^+\tau^-$ , has been used to search for the neutral MSSM Higgs boson.

If a single bottom quark is tagged then the final state is  $bh$  or  $\bar{b}h$  (the curve labelled '1 b'). A recent Tevatron study [?] used the search for neutral MSSM Higgs bosons in events with three bottom quarks in the final state ( $bh^0 + \bar{b}h^0$  production with  $h^0 \rightarrow b\bar{b}$ ) to impose limits on the  $\tan\beta$  and  $M_{A^0}$  parameter space.

Finally, we show the fully exclusive cross sections for  $b\bar{b}h$  production, where both the outgoing  $b$  and  $\bar{b}$  quarks are identified (the curve labelled '2 b').

---

<sup>1</sup>We assume  $M_{SUSY} = 1$  TeV,  $M_{\tilde{g}} = 1$  TeV,  $A_b = A_t = 2$  TeV ( $h^0$ ),  $A_b = A_t = 25$  GeV ( $H^0$ ),  $\mu = M_2 = 200$  GeV ( $h^0$ ), and  $\mu = M_2 = 1$  TeV ( $H^0$ ). For  $M_{h^0} = 120$  GeV, the  $bbh^0$  coupling is enhanced by a factor of 33 relative to the SM coupling, while for  $M_{H^0}$  between 200 and 800 GeV, the  $bbH^0$  coupling is enhanced by a factor of 27 relative to the SM coupling.

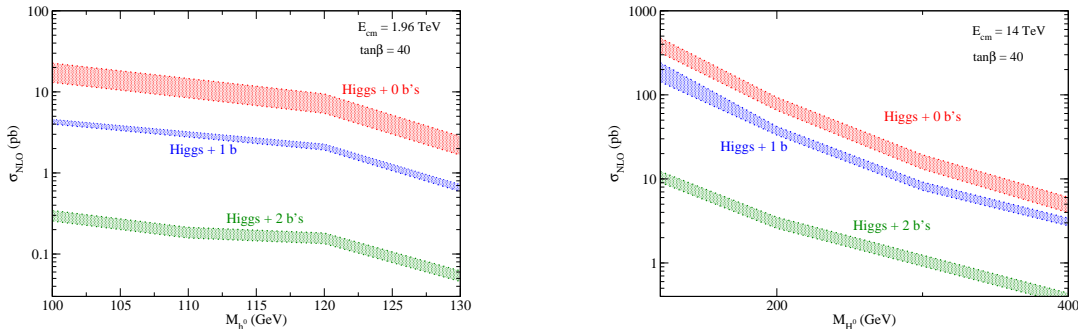


Figure 2: Total cross sections for  $pp, p\bar{p} \rightarrow (b\bar{b})h$  in the MSSM in the 4FNS at NLO for the Tevatron and the LHC in the MSSM with  $\tan\beta = 40$ . The Tevatron (LHC) plot is for the lightest (heaviest) neutral Higgs boson,  $h^0$  ( $H^0$ ). The error bands have been obtained by varying the renormalization and factorization scales as described in the text.

## Differential Cross Sections for Associated $b$ Higgs Production

In comparing the four and five flavor number schemes it is particularly interesting to compare the kinematic distributions. In Figs. 3-4, we compare the results for the NLO transverse momentum and pseudorapidity distributions of the light and heavy MSSM Higgs bosons,  $h^0$  and  $H^0$ , in both the 4FNS and 5FNS, at the Tevatron and the LHC. We see, in general, good agreement between the two schemes within their respective theoretical uncertainties, except in regions of kinematic boundaries. This is particularly dramatic in the  $p_T^h$  distributions in the 5FNS where, around  $p_T^h \simeq 20$  GeV, a kinematic threshold induced in  $bg \rightarrow bh$  by the cut on the  $p_T$  of the bottom quark causes the 5FNS NLO calculation to be unreliable.

Finally, in Figs. 5 and 6 we illustrate the impact of NLO QCD corrections on the transverse momentum and pseudorapidity distribution of the SM Higgs boson and the bottom quark by showing the relative correction,  $d\sigma_{NLO}/d\sigma_{LO} - 1$  (in percent) for the exclusive case ( $b\bar{b}h$  where both  $b$  quarks are observed). For the renormalization/factorization scale we choose  $\mu = 2\mu_0$  at the Tevatron and  $\mu = 4\mu_0$  at the LHC. As can be seen, the NLO QCD corrections can considerably affect the shape of kinematic distributions, and their effect cannot be obtained from simply rescaling the LO distributions with a K-factor of  $\sigma_{NLO}/\sigma_{LO} = 1.38 \pm 0.02$  (Tevatron,  $\mu = 2\mu_0$ ) and  $\sigma_{NLO}/\sigma_{LO} = 1.11 \pm 0.03$  (LHC,  $\mu = 4\mu_0$ ). The kinematic distributions have been calculated within the Standard Model and using the on-shell scheme for the definition of the  $b$  quark mass, but we see a similar behavior when using the  $\overline{MS}$  bottom quark Yukawa coupling.

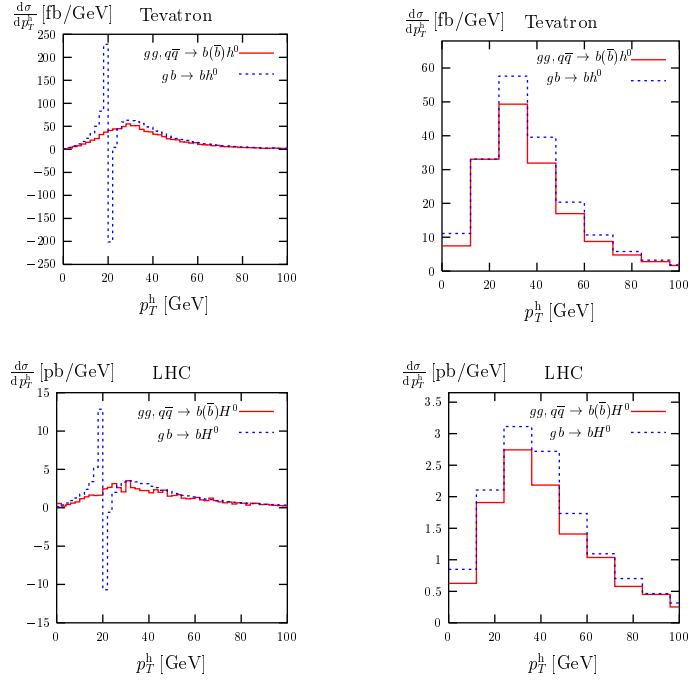


Figure 3:  $d\sigma/dp_T^h$  in the MSSM at the Tevatron and the LHC for  $M_{h^0, H^0} = 120$  GeV and  $\mu_r = \mu_F = \mu_0/2$  for single  $b$ -tag events. We show the NLO results in the 4FNS (solid) and 5FNS (dashed), using two different bin sizes, 2 GeV (left) and 12 GeV (right).

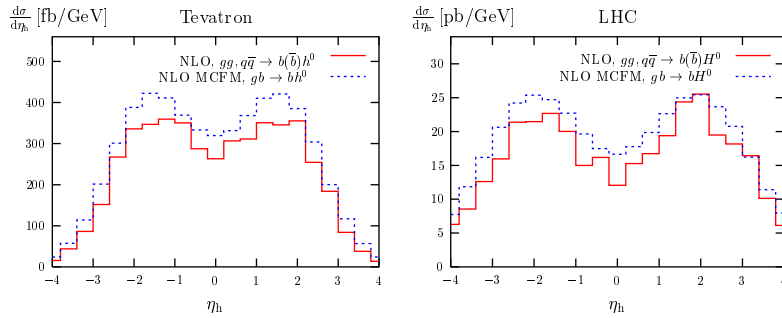


Figure 4:  $d\sigma/d\eta_h$  in the MSSM at the Tevatron and the LHC for  $M_{h^0, H^0} = 120$  GeV and  $\mu_r = \mu_f = \mu_0/2$  for single  $b$ -tag events. We show the NLO results in the 4FNS (solid) and 5FNS (dashed).

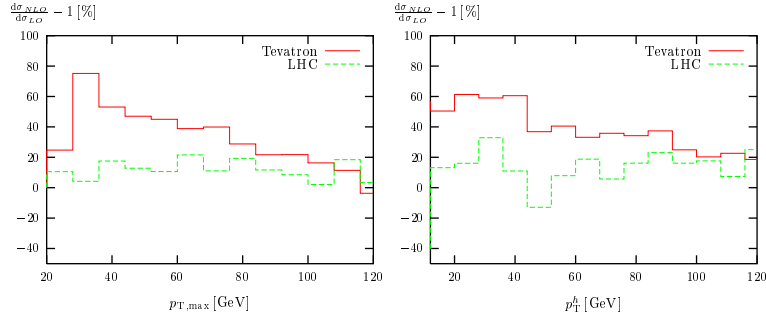


Figure 5: The relative corrections  $d\sigma_{NLO}/d\sigma_{LO} - 1$  for the  $p_T$  distribution of the bottom or anti-bottom quark with the largest  $p_T$  ( $p_{T,max}$ ) (left) and of the SM Higgs boson ( $p_T^h$ ) (right) to  $b\bar{b}h$  production in the SM at the Tevatron (with  $\sqrt{s} = 2$  TeV and  $\mu = 2\mu_0$ ) and the LHC (with  $\sqrt{s} = 14$  TeV and  $\mu = 4\mu_0$ ).

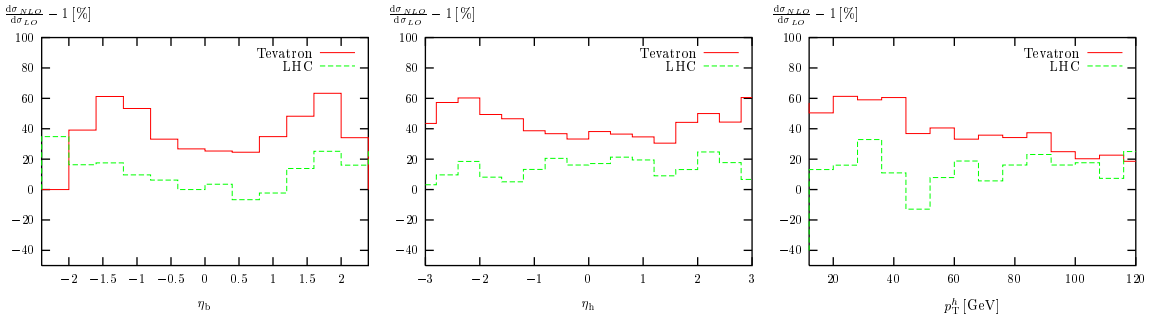


Figure 6: The relative corrections  $d\sigma_{NLO}/d\sigma_{LO} - 1$  for the  $\eta$  distribution of the bottom quark  $\eta_b$  (left) and of the SM Higgs boson ( $\eta_h$ ) (right) to  $b\bar{b}h$  production in the SM at the Tevatron (with  $\sqrt{s} = 2$  TeV and  $\mu = 2\mu_0$ ) and the LHC (with  $\sqrt{s} = 14$  TeV and  $\mu = 4\mu_0$ ).

## PDF and Renormalization/Factorization Scale Uncertainties

A major source of theoretical uncertainty for cross section predictions comes from the PDFs. We study the uncertainties of semi-inclusive  $b\bar{b}h$  production rates that come from the uncertainties in the PDFs using the CTEQ PDF sets. First, the central value cross section  $\sigma_0$  is calculated using the global minimum PDF (i.e. CTEQ6M). The calculation of the cross section is then performed with the additional 40 sets of PDFs to produce 40 different predictions,  $\sigma_i$ . For each of these, the deviation from the central value is calculated to be  $\Delta\sigma_i^\pm = |\sigma_i - \sigma_0|$  when  $\sigma_i \gtrless \sigma_0$ . Finally, to obtain the uncertainties due to the PDFs the deviations are summed quadratically as  $\Delta\sigma^\pm = \sqrt{\sum_i \Delta\sigma_i^{\pm 2}}$  and the cross section including the theoretical uncertainties arising from the PDFs is quoted as  $\sigma_0|_{-\Delta\sigma}^{+\Delta\sigma}$ .

In Figs. 7 and 8 we plot the total SM NLO cross section for  $bg \rightarrow bh$  at the

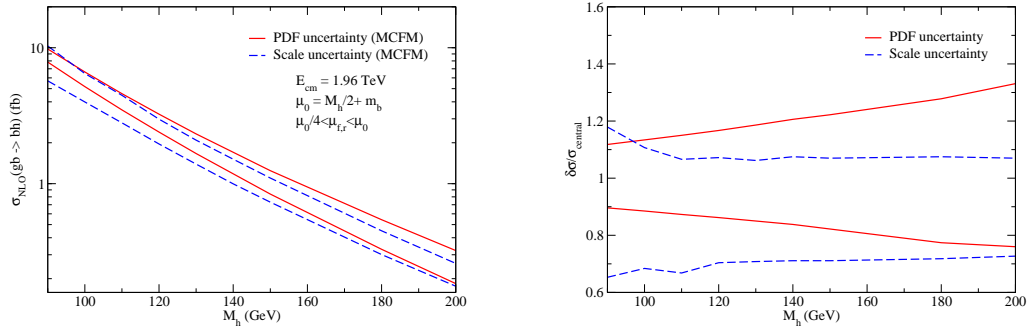


Figure 7: Comparison between theoretical uncertainties due to scale dependence and uncertainties arising from the PDFs at the Tevatron for semi-inclusive  $bh$  production in the Standard Model. In the bottom plot, both uncertainty bands have been normalized to the central value of the total cross section  $\sigma_0$ .

Tevatron and LHC respectively. Here, we compare the uncertainties from residual scale dependence and the PDFs both for the total cross section (left) and the total cross section normalized to the central value calculated with CTEQ6M (right).

From Fig. 8 one can see that, at the LHC, the theoretical uncertainty is dominated by the residual scale dependence. Due to the large center of mass (c.o.m.) energy of the LHC, the gluons and bottom quarks in the initial state have small momentum fraction ( $x$ ) values and, hence, small PDF uncertainties typically in the 5-10% range.

In contrast, due to the smaller c.o.m. energy, the PDF uncertainties at the Tevatron (Fig. 7) are comparable and even larger than the uncertainties due to residual scale dependence over the full Higgs mass range. The smaller c.o.m. energy results in higher- $x$  gluons and bottom quarks in the initial state which corresponds to large PDF uncertainties in the 10-30% range.

## 1.4 Conclusion

## Acknowledgments

The work of S.D. and C.J. ( L.R) is supported in part by the U.S. Department of Energy under grant DE-AC02-98CH10886 (DE-FG-02-91ER40685). The work of D.W. is supported in part by the National Science Foundation under grant No. PHY-0244875.

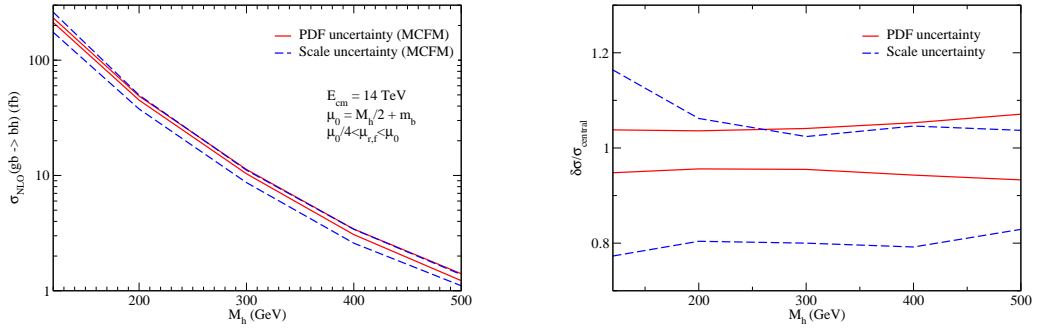


Figure 8: Comparison between theoretical uncertainties due to scale dependence and uncertainties arising from the PDFs at the LHC for semi-inclusive  $bh$  production in the Standard Model. In the bottom plot, both uncertainty bands have been normalized to the central value of the total cross section  $\sigma_0$ .

